Fluctuations in the Local Rate of Turbulent Mass Transfer to a Pipe Wall

PAUL VAN SHAW and THOMAS J. HANRATTY

University of Illinois, Urbana, Illinois

The major resistance to transfer of mass between a fluid in fully developed turbulent flow and a pipe wall is confined to a thin layer of fluid adjoining the surface. In early attempts to describe the resistance to transfer it was assumed that there is a region adjoining the surface throughout which the fluid behaves as if it were in laminar motion (*1*). If this hypothetical laminar layer were to represent the entire resistance to transfer, the rate of transfer to the surface would be given as

$$J = D(C_b - C_w)/\delta_c \qquad (1)$$

It is well established that there is a portion of the flow field ($y^+ < 5$) where indeed the average velocity profile is described by the equation of rectilinear laminar motion, even through the flow in this region is highly disturbed. If the thickness of this viscous sublayer is substituted for δ_c in Equation (1), low rates of material transport are predicted at high Schmidt numbers. The concentration profile need not be linear throughout $y^+ < 5$, and virtually the entire change in concentration may be confined to a much thinner region. Therefore in order for the laminar film model to be applicable, δ_c must be a function of the Schmidt number.

The lack of correspondence between the thickness of the viscous sublayer and the diffusion layer δ_c arises because the flow within the region $y^+ < 5$ is actually unsteady. This has long been recognized by fluid dynamicists and has been amply demonstrated (*2, 7, 9*). The nature of the unsteady flow near a wall has been discussed in a recent paper by Sternberg (*13*). Apparently the character of wall turbulence is such that even though it is of relatively high intensity, it does not significantly influence the transfer of momentum within the region $y^+ < 5$. However molecular transport of mass at high Schmidt numbers is much less effective than molecular transport of momentum, so that even a low level of the turbulence may exert a significant influence on material transport. Therefore theoretical analyses of the process of turbulent exchange of a scalar quantity should allow for the effect of turbulence right to the wall.

Since the flow field is unsteady in the immediate vicinity of the transfer surface, one would expect the local mass transfer rate to fluctuate in time. In order to examine the effect of such fluctuations on the average mass transfer rate, Hanratty (*3*) developed a model which is the antithesis of the laminar film model, one which predicts chaotic fluctuations in the mass transfer coefficient [$(\overline{k^2})^{1/2}/\overline{K} = \infty$]. In this work the surface renewal or penetration concept of Danckwerts, which hypothesizes periodic or random replacement of fluid elements in contact with the wall by fresh elements, was used to describe turbulent exchange with a channel or a pipe wall. This type of treatment has been generalized in recent articles (*4, 14*).

It is evident that neither the laminar film model nor the surface renewal model are satisfactory since they do not yield a quantitative relationship between the concentration field and the unsteady flow field in the vicinity of a solid surface. Experimentation has been needed which will give insight into the nature of this relation and which will determine the degree to which the various models determine reality. Reiss and Hanratty (*8, 9*) recently described experiments in which they measured average and fluctuating rates of transfer of mass to small circular area elements in an inert wall. The transfer elements were the tips of nickel wires inserted through holes in the wall of a plastic pipe and smoothed flush with the wall. An electrochemical reaction was carried out on the wire tips in such a manner that the reaction rate was controlled by the rate of diffusion of ions to the surface. Their technique provides a means of investigating the mechanics of turbulent exchange with a wall. This paper describes the results of such an investigation.

The present experimental scheme differs from that of Reiss and Hanratty in that the test electrodes, instead of being surrounded by inert surface, are surrounded by active electrode surface. The arrangement provides a means of measuring the instantaneous rate of transfer to a small area element of a relatively large transfer surface. Measurements are presented of the root-mean-square, the frequency spectra, and the scale of the fluctuations in the local mass transfer coefficients. Measurements of local time average rates of mass transfer are presented to demonstrate the validity of the experimental technique. All of the measurements are for fully developed flow and fully developed mass transfer at a Schmidt number of approximately 2,400 and a Reynolds number range of 10,000 to 60,000.

A previous publication by the authors and L. Philip Reiss (*12*) presents a certain amount of background information pertinent to the present study. This reference describes how the Schmidt number for the system was obtained and indicates the length of transfer section required for the mass transfer to become fully developed.

DESCRIPTION OF EXPERIMENTS

The system used in the experiments reported here is similar to that described in reference *12*. The techniques employed have previously been described in detail (*8, 9, 11, 12*), and only a brief description given here.

The electrolytic cell, which is illustrated schematically in Figure 1, consisted of three (or more) electrodes on the inner wall of a pipe through which an electrolyte was pumped. An 11 cm. long, axially symmetric, nickel control electrode, cut from a length of 1-in. I.D. nickel pipe, formed the main portion of the mass transfer surface. One or more test electrodes consisting of nickel wires were inserted through holes in the wall of the control electrode and cemented in place. These were smoothed flush with the inner surface of the control electrode so that only their tips were exposed. A 5 ft. long section of 1-in. I.D. nickel pipe, mounted downstream of the composite electrode described above, served as the reference electrode for the cell reaction.

Paul Van Shaw is with the University of California, Davis, California.

In operation a potential difference was applied between the reference electrode and the control and test electrodes (with separate circuits used for the control and test electrodes), and the following reactions were carried out:
Control and test electrodes

$$(\text{cathodes}) : Fe(CN)_6^{-3} + e \rightarrow Fe(CN)^{6-4}$$

Reference electrode (anode) : $Fe(CN)^{6-4} \rightarrow Fe(CN)_6^{-3} + e$

The current flowing in a given electrode circuit was a direct measure of the rate of reaction on the associated electrode. Thus it was possible to determine the rate of reaction on a given test electrode independently of the overall reaction rate.

If the applied potential difference is sufficiently high, the concentration of the reacting species on the cathode surface is essentially zero and the rate of reaction is controlled by the rate of transport of ferricyanide ions to the cathode surface. In general transport of ions to an electrode surface occurs not only as a result of diffusion but also as a consequence of migration under the influence of the electric field surrounding the surface The latter mechanism however was effectively eliminated in the reported experiments by the presence of a high concentration of inert ions in the electrolyte. The electrolyte consisted of a 2 molar sodium hydroxide solution with $\sim 10^{-3}$ molar concentrations of ferri and ferrocyanide ions.

Local rates of mass transfer to the electrode surface were measured on the tips of test electrodes with diameters of 0.0159, 0.0259, 0.064, and 0.125 in. The hole drilled in the control electrode to accommodate these wires were drilled from two to three thousandths of an inch oversize. The space between a given wire and the wall of the hole in which it was mounted was carefully filled with cement to insure that the wire was electrically insulated from the control electrode. All the test electrodes were sufficiently far downstream of the leading edge of the control electrode that the mass transfer process was fully developed in their vicinity.

The control electrode was preceded in the flow loop by approximately 18 ft. of straight 1-in. I.D. plastic pipe. Discontinuities at joints were carefully eliminated so that the flow through the cell could be considered fully developed. The inner surface of the electrolytic cell was sanded and polished with progressively finer grades of emery paper so that the walls could be considered to be hydraulically smooth.

A negative potential relative to that of the reference electrode was applied to the control and test electrodes with the independent external circuits shown in Figure 2 and described in the following section. When the applied potential was sufficiently high, the current in each circuit was proportional to the rate of diffusion of ferricyanide ions to the electrode surface. This proportionality is expressed as

$$J = \frac{I}{AF} \tag{2}$$

Since the concentration of ferricyanide ions in the electrolyte varied somewhat from run to run, it is convenient to define a mass transfer coefficient K as

$$K = \frac{J}{C_b - C_w} = \frac{J}{C_b} \tag{3}$$

with $C_w = 0$ when the electrode reaction is diffusion controlled. With turbulent flow over the electrode surface it is

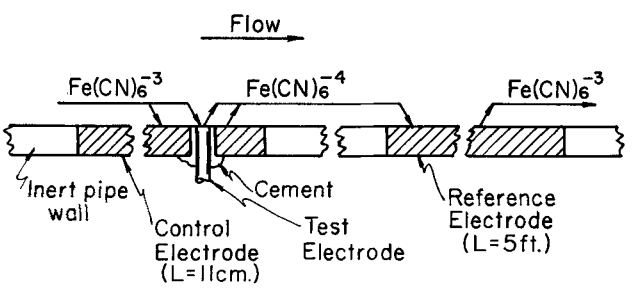

Fig. 1. Schematic representation of electrode system.

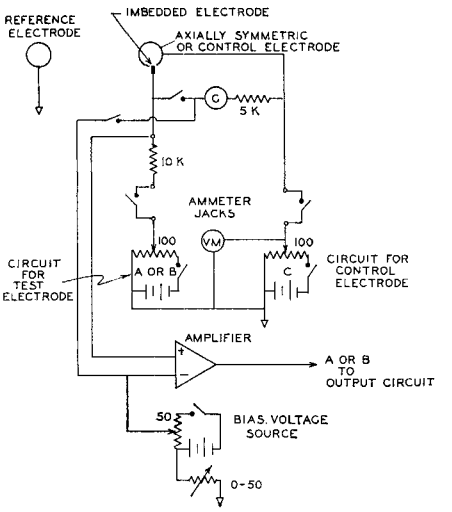

Fig. 2. Electrode circuits.

found that the mass transfer coefficient has both an average and a fluctuating component $K = \overline{K} + k$, where $\overline{K}$ and k are directly related to the time average of and the fluctuations in the current flowing in the test electrode circuit.

The magnitude of the fluctuations in the mass transfer coefficient may be described in terms of a mass transfer intensity defined by the ratio $(\overline{k^2})^{1/2}\ \overline{K}$, where

$$\overline{k^2} = \lim \frac{1}{T} \int_o^T k^2 dt \tag{4}$$

$$T \rightarrow \infty$$

The frequencies of the fluctuations of the mass transfer rate can be related to a spectral density function $F_k(n)$ which has the property

$$\overline{k^2} = \int_o^\infty F_k(n) dn \tag{5}$$

Spectral measurements are reported in the form of integral frequency distribution functions $f(n)$, where

$$f(n) = \frac{\int_o^n F_k(n) dn}{\overline{k^2}} \tag{6}$$

The value of n at which $f(n) = 0.5$ could be looked upon as the average frequency of the fluctuations. It should be noted that in practice, because of the characteristics of the band pass filters used in the study, the lower limit in the last two integrals was not 0 but 0.02 cycles/sec. It is assumed that the contribution of mass transfer fluctuations with frequencies of less than 0.02 cycles/sec. to the total is negligible.

By simultaneously measuring the current through the circuits of two test electrodes a correlation coefficient R may be measured, where

$$R = \frac{\overline{k_1\ k_2}}{(\overline{k_1^2\ k_2^2})^{1/2}} \tag{7}$$

Two types of spatial correlation coefficients were determined; longitudinal R_a in which the two test electrodes lay on a line parallel to the pipe axis, and circumferential R_c in which they were located on the same pipe circumference. By measuring these correlation coefficients for different distances between the test electrodes the extent of the fluctuations in the longitudinal and in the circumferential directions can be described in terms of longitudinal and circumferential integral scales:

$$\lambda_a = \int_o^\infty R_a dx \tag{8}$$

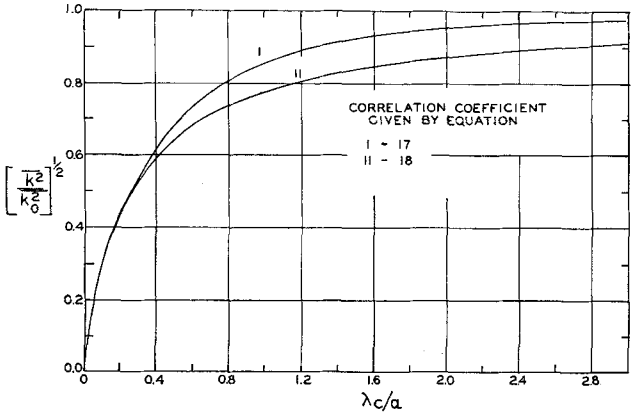

Fig. 3. Calculated nonuniform field correction.

$$\lambda_c = \int_o^\infty R_c dz \tag{9}$$

ELECTRODE CIRCUITS

Figure 2 shows a diagram of the circuit used with the control electrode and a diagram of one of the two identical circuits constructed for use in conjunction with imbedded electrodes. The circuit for the control electrode provides the means to apply the electrode potential and to measure the average current. The circuit for the imbedded electrode provides for the application of the electrode potential and the measurement of the average electrode current. It also converts the current fluctuations to amplified voltage fluctuations. The potential applied to the test electrodes was not measured directly but was equated to the potential of the control electrode by means of a galvanometer connected across the two leads.

A 10,000-ohm precision resistor in series with the imbedded electrode converted current fluctuations to voltage fluctuations. The fluctuating voltage was amplified with a wide band, differential input amplifier which provides gains of up to approximately 10,000. The amplifier output was the amplified difference between two input potentials, one of which was set equal to the average potential of the test electrode by means of the bucking voltage circuit indicated in the diagram.

The characteristics of the fluctuations in the test electrode currents (fluctuations in the local mass transfer coefficients) were determined with a random signal voltmeter correlator that was specially constructed for this study from analogue computer components. The unit was designed for the simultaneous calculation of the mean square of one fluctuating input potential and the mean product of two inputs over time intervals of up to 2 min. Longer averaging times were obtained by iteration. The same unit, coupled with variable range band pass filters, served for the spectral analyses.

CORRECTION FOR ERRORS RESULTING FROM USE OF A TEST ELECTRODE WITH A FINITE AREA

No probe of finite size can provide true measurements of local fluctuations in a field. Errors of considerable magnitude result from averaging of the effects of the disturbances over the surface of the probe if its dimensions are not small compared with the scale of the disturbances. The results of this study and others (*6*, 9), indicate that the scale of turbulence in the wall region is large in the direction of the mean flow but quite small in the transverse direction. As a result, it is found that measured mass transfer intensities depend quite strongly on the diameter of the imbedded electrode used in making the measurement. In order to estimate the true local mass transfer intensity it is necessary to develop a means of correcting for the finite size of the electrode.

The representation of the electrode for the development of such a correction is as follows. The circular test electrode has a radius a and is centered at the origin of a plane cartesian coordinate system with the x direction taken as the direction of the mean flow. The electrode surface is divided into strips of width Δz centered about z_i and running parallel to the x axis. It is assumed that the concentration and flow fields over any strip are uniform.

The fluctuating component of the rate of mass transfer to any strip is

$$q_i = 2k_i C_b \Delta z (a^2 - z_i^2)^{1/2} \tag{10}$$

The fluctuating component of the rate of transfer to the entire surface of the test electrode is given by the sum of the components q_i over the surface. The mean square of the fluctuations is

$$\overline{Q^2} = 4C_b^2 \sum_i \sum_j \overline{k_i k_j} \left[(a^2 - z_i^2)(a^2 - z_j^2) \right]^{1/2} \Delta z_i \Delta z_j \tag{11}$$

When one recalls the definition of the correlation coefficient, the above equation may also be written as

$$\overline{Q^2} = 4C_b^2 \overline{k_o^2} \Sigma_i \Sigma_j R_{i,j} \left[(a^2 - z_i^2)(a^2 - z_j^2) \right]^{1/2} \Delta z_i \Delta z_j \tag{12}$$

If on the other hand the fields over the test electrode surface were uniform, the expression for $\overline{Q^2}$ would be simply

$$\overline{Q^2}_{\text{uniform}} = \Pi^2 a^4 \overline{k_o^2} C_b^2 \tag{13}$$

When one notes that the measured mass transfer fluctuations are

$$\overline{Q^2} = \Pi^2 a^4 \overline{k^2} C_b^2 \tag{14}$$

where k is the fluctuating mass transfer coefficient averaged over the surface of the test electrode, the desired correction factor is given by

$$\overline{k^2}/\overline{k_o^2} = (4/\Pi^2 a^4) \Sigma_i \Sigma_j R_{i,j} \left[(a^2 - z_i^2)(a^2 - z_j^2) \right]^{1/2} \Delta z_i \Delta z_j \tag{15}$$

Introducing $y = z/a$ and passing to the limit as $\Delta y \to 0$, the above relation

$$\overline{k^2}/\overline{k_o^2} = (4/\Pi^2) \int_{-1}^{1} \int_{-1}^{1} R_{i,j} \left[(1 - y_i^2)(1 - y_j^2) \right]^{1/2} dy_i dy_j \tag{16}$$

The development is at this point somewhat arbitrary because of the necessity of introducing an assumption regarding the variation of the circumferential correlation coefficient with y. Figure 3 shows correction factors for the two assumed distributions:

$$R_{i,j} = \exp\left[- |y_i - y_j| / (\lambda_c/a) \right] \tag{17}$$

Table 1. Local Time Average Mass Transfer Coefficients, Fully Developed Transfer

Imbedded electrode diameter	K_∞+ (least squares average)	Number of measurements averaged	Maximum deviation from average
0.0159 in.	3.02×10^{-4}	6	2%
0.0259 in.	3.02×10^{-4}	12	4
0.064 in.	2.97×10^{-4}	5	3
0.125 in.	3.00×10^{-4}	6	3
Overall Average	3.01×10^{-4}	29	

TABLE 2. CIRCUMFERENTIAL INTEGRAL SCALES

Reynolds number	λ_c, cm.	$\lambda_c^+ = \frac{\lambda_c U^*}{\nu}$
10,000	0.010	2.47
22,000	0.005	2.47
30,000	0.004	2.60
60,000	0.002	2.38

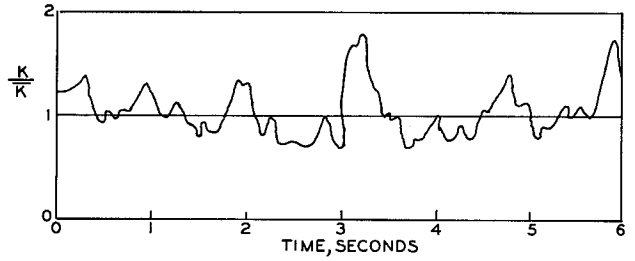

Fig. 4. Variation of fully developed mass transfer coefficient with time, $N_{Re} = 19{,}700$.

$$R_{i,j} = \exp\left[-(y_i - y_j)^2/(\lambda_c/a)^2\right] \qquad (18)$$

The calculated correction factors are applied to the measured values of $\overline{k^2}$ by trial and error; that is, one guesses values of λ_c until one obtains agreement between mass transfer intensities measured using different sized test electrodes.

EXPERIMENTAL RESULTS

Local time average mass transfer coefficients were directly measured with imbedded test electrodes at least three pipe diameters downstream of the leading edge of the control electrode. In accordance with the results presented in reference *12* the mass transfer process should be fully developed at that distance into the transfer section. Thus the measured time average local mass transfer coefficients $\overline{K}$ should be independent of position and Reynolds number when expressed as the dimensionless ratio

$$K_\infty^+ = \frac{\overline{K}}{U^*}$$

This is indeed the behavior shown by the data summarized in Table 1, which represent measurements taken over the Reynolds number range of from 9,700 to 60,100. Certain of the measurements summarized in Table 1 were made with electrodes mounted on both the sides and the bottom of the horizontal test section. Since no dependence

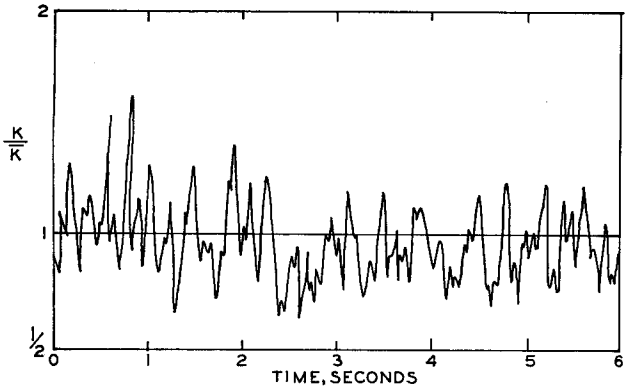

Fig. 5. Variation of fully developed mass transfer coefficient with time, $N_{Re} = 48{,}100$.

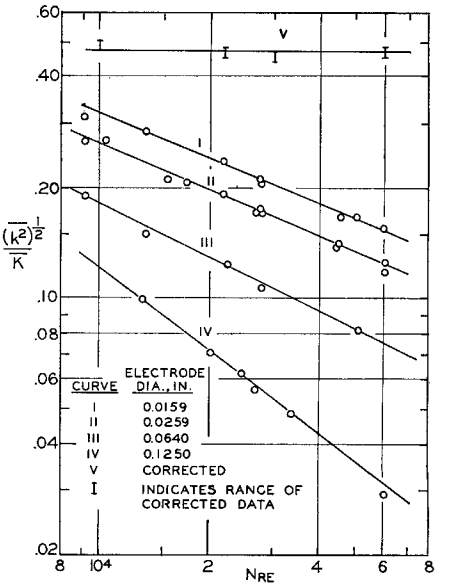

Fig. 6. Variation of mass transfer intensity with Reynolds numbers.

of the results upon circumferential position could be noted, it is evident that natural convection effects are unimportant.

Oscillograms showing the time dependence of the rate of transfer of mass to an imbedded electrode with a diameter of 0.0259 in. at two different Reynolds numbers are shown in Figures 4 and 5. They are included to illustrate the qualitative nature of the fluctuations. It is important to keep in mind that they represent fluctuations in the rate of transfer of mass to a finite area of the transfer surface rather than to a true point on the surface. Because the effects of fluctuations of smaller scale than the test electrode diameter tend to be averaged over the surface, the oscillograms display fluctuations of attenuated magnitude.

Figure 6 shows the measured mass transfer intensity as a function of Reynolds number for four different test electrode diameters. A curve has been added to the figure to show the appearance of the data after application of the correction for the finite size of the electrodes. The four sets of data were brought into agreement with the exponential relation for the correlation coefficient distribution [Equation (17)] with the circumferential integral scales shown in Table 2.

The mass transfer intensity data were found to be reproducible to within 6%. As in the case of the average measurements the results were independent of the circumferential positions of the imbedded electrodes.

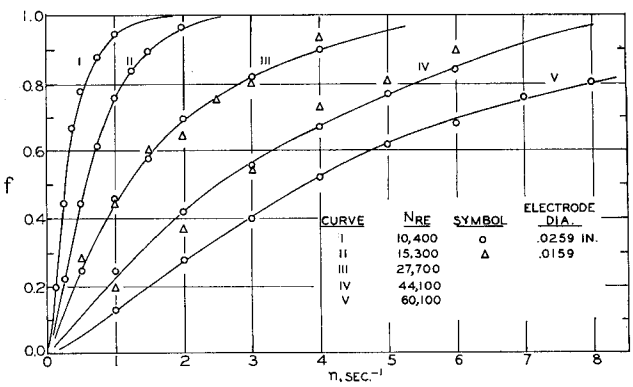

Fig. 7. Integral frequency distribution of mass transfer fluctuations.

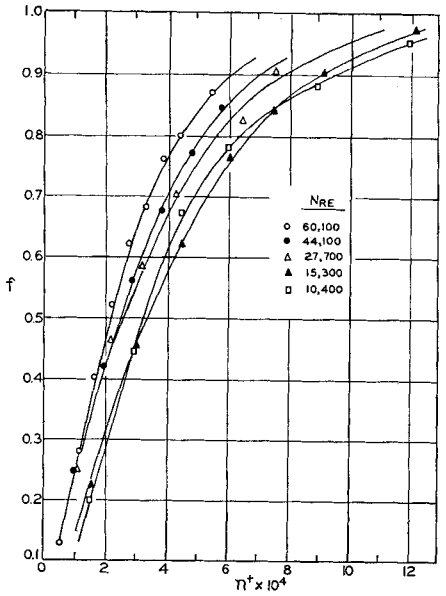

Fig. 8. Frequency distributions correlated on the law of the wall time scale.

The oscillograms presented in the preceding section show that the frequency of the mass transfer fluctuations is strongly dependent on the Reynolds number. This dependence is shown quantitatively by Figure 7, a plot of the integral frequency distribution function f against the frequency n for several Reynolds numbers. Virtually all the spectral data were obtained with test electrodes with diameters of 0.0259 in. Two runs however were reproduced with the smaller sized electrodes in order to determine the effect of electrode size on the measurements. In Figure 8 the spectral data are plotted against the dimensionless frequency $n^+ = nv/U^{*2} = n\left(\frac{\overline{du}}{dy}\right)_w^{-1}$.

Axial correlation coefficients measured with two imbedded electrodes with diameters of 0.0259 in. spaced from 5 to 30 mm. (center to center) apart along a line parallel to the pipe axis are presented in two graphical forms. Figure 9 shows the data in the form of a plot of the correlation coefficient $R_{1,2}$ against the electrode separation $(x_1 - x_2)$. Figure 10 shows the same data plotted against the dimensionless electrode separation $(x_1^+ - x_2^+)$. Longitudinal integral scales of the fluctuations were determined by graphical integration of the areas under the curves shown in Figure 9. The values thus determined are presented in Table 3.

A set of simultaneously recorded oscillograms of mass transfer fluctuations at two imbedded electrodes 5 mm. apart on a line parallel to the pipe axis were obtained

Table 3. Longitudinal Integral Scales

Reynolds number	λ_a, pipe diameters	$\lambda_a^+ = \frac{\lambda_a U^*}{\nu}$
10,400	0.54	354
15,300	0.36	330
27,700	0.28	429
44,100	0.19	436
60,100	0.16	484

(Figure 12). If one pictures the fluctuations as being caused by a wavelike disturbance moving downstream, a disturbance velocity may be obtained by measuring the horizontal displacement of corresponding peaks and valleys on the two simultaneously recorded oscillograms. Disturbance velocities thus estimated for two Reynolds numbers are compared with the friction velocity and bulk velocity in the presentation below.

Reynolds number	Disturbance velocity, cm./sec.	Friction velocity, cm./sec.	Bulk velocity, cm./sec.
15,900	4.5	4.6	77.5
21,000	6.3	5.6	102.4

It is emphasized that the disturbance velocities presented above must be considered as estimates. They are in fact averages of a large number of individual determinations which deviated as much as plus or minus 50% from the average.

An attempt to measure circumferential correlation coefficients with the electrode pair technique was unsuccessful. No measureable correlation was observed between the fluctuations at two imbedded electrodes just 2.5 mm. apart on a pipe circumference. This result is consistent with the mass transfer intensity measurements and the small circumferential integral scales obtained as by-products of the application of the nonuniform field correction.

Frequency spectra of velocity fluctuations in the direction of the mean flow and of pressure fluctuations at the wall are compared with mass transfer spectra in Figure 11. In addition to the mass transfer data of the present study the figure shows the data obtained by Reiss and Hanratty (9) for fluctuations in the rate of transfer of mass to an isolated sink on a pipe wall. (These reflect fluctuations in the wall shear stress.) The ordinate is the dimensionless spectral density function defined as

$$\frac{2U_b}{d} F_k(n)/\overline{k^2} \text{ for mass transfer}$$

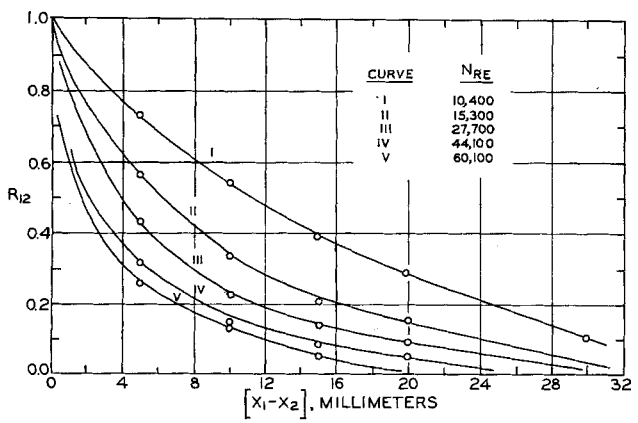

Fig. 9. Variation of axial correlation coefficient with separation.

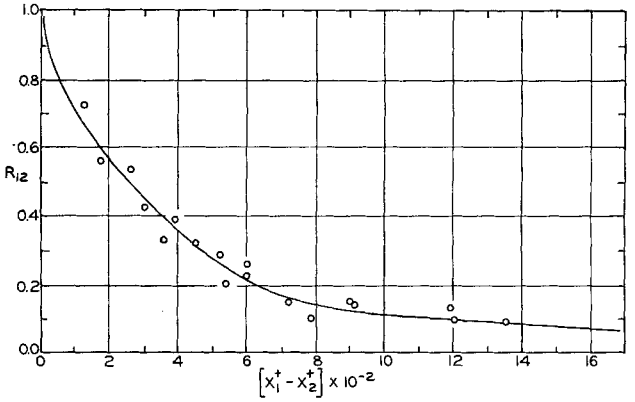

Fig. 10. Variation of axial correlation coefficient with dimensionless separation.

$$\frac{2U_b}{d} F_p(n)/\overline{p^2} \text{ for pressure}$$

and

$$\frac{2U_b}{d} F_u(n)/\overline{u^2} \text{ for velocity}$$

The abscissa is the dimensionless frequency $nd/2U_b$. In order to obtain the spectral density function for the mass transfer data of the present study the integral frequency distribution was fitted by an exponential curve and then differentiated.

DISCUSSION OF RESULTS

Measurements of time average local rates of mass transfer have been presented here for two reasons. First the measurements are of interest in themselves because they are directly measured local average mass transfer measurements. In this respect it is notable that these results are in complete agreement with the correlation presented by the authors in a previous publication (*12*). At high Schmidt numbers the dimensionless mass transfer coefficient $K^+ = \overline{K}(X)/U^*$ approaches a constant value independent of Reynolds number and position for sufficiently large X. The limiting value obtained in the study reported here is identical to that previously reported. The second reason for including these results is to show that the imbedded electrodes do act as extensions of the control electrode surface. In other words the results indicate that the discontinuity in the electrode surface which surrounds the imbedded test electrodes is not sufficient to upset the developed average concentration profile.

The most striking results of this research are the very large magnitude of the fluctuations in the mass transfer rate, the relative sizes of the longitudinal and circumferential scales, and the low frequency of the mass transfer fluctuations. The oscillograms as well as the value of $\frac{(\overline{k^2})^{1/2}}{\overline{K}} \cong 0.47$ calculated from the measurements show that the fluctuations in the mass transfer rate are of approximately the same magnitude as the time averaged mass transfer rate. This presents a picture which clearly indicates the chaotic nature of the process of turbulent mass transfer.

Both the circumferential correlation measurements and the nonuniform field corrections show that the scale of

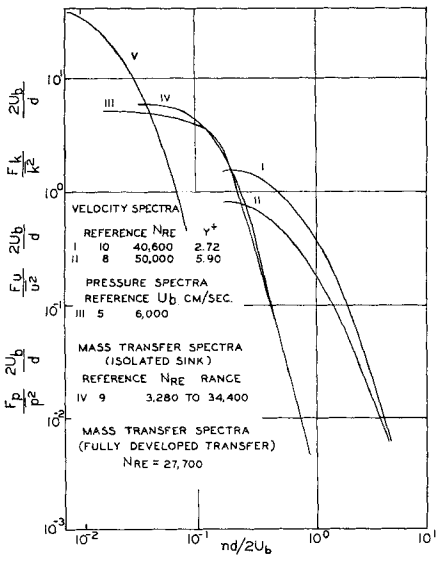

Fig. 11. Comparison of mass transfer, velocity, and pressure spectra.

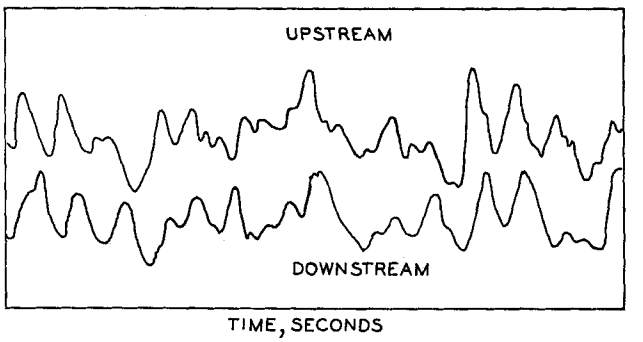

Fig. 12. Fluctuations in the rates of mass transfer to two imbedded electrodes 5 mm. apart on a line parallel to the pipe axis, N_{Re} = 21,000.

the fluctuations in the circumferential direction is quite small. In fact the result $\lambda_c^+ \cong 2.5$ suggests that it is of the same magnitude as the thickness of the diffusion layer. Longitudinal scales are two orders of magnitude larger than the circumferential scale ($\lambda_a^+ \cong 400$). One therefore obtains a picture of a spaghettilike disturbance field. The elongation of disturbances at the wall in the flow direction has also been noted in measurements of wall shear stress fluctuations by Reiss and Hanratty (*9*) and in the dye streak observations of Kline and Runstadler (*6*). However it is to be noted that the circumferential scales suggested by the results of this research are much smaller than those indicated by the latter two investigations. This suggests that these different studies reflect different aspects of the fluctuating flow field close to the wall. This is discussed in the next section of this article, where it is pointed out that flow fluctuations in the direction of mean flow which play a dominant role in the phenomenon studied by Reiss and Hanratty have a negligible influence on the results reported in this paper.

The low characteristic frequency of the mass transfer fluctuations is clearly shown in Figure 11, where the frequency spectra of mass transfer fluctuations, pressure fluctuations, and velocity fluctuations are compared. It is also evidenced by the low velocity of the disturbance field estimated from the oscillograms as compared with that for pressure fluctuations.

The disturbance velocity is approximately equal to the friction velocity; that is the local average velocity at $y^+ = 1$. This would correspond to the mean velocity at a point in the central part of the concentration boundary layer. The disturbance velocity for pressure fluctuations and for shear stress fluctuations on the other hand is found to be approximated by the bulk average fluid velocity.

The very high intensity of the mass transfer fluctuations and their low characteristic frequency suggest that a surface renewal model might provide a rough approximation of the mass transfer process. It is therefore of interest to compare the measured average mass transfer coefficients with values obtained if one assumes the most simple type of surface renewal model. Hanratty (*3*) has shown that if it is assumed that the fluid in contact with the wall is replaced at fixed time intervals T_c by fluid of bulk concentration, the average rate of mass transfer to the surface is given by

$$\overline{K} = 2(\nu/T_c N_{Sc}\,\Pi)^{1/2} \qquad (19)$$

The following is a comparison of measured average mass transfer coefficients to values calculated from the above relation with the measured mean frequencies substituted for $1/T_c$. The value of the Schmidt number is taken to be 2,400 (*12*).

Reynolds number	Measured K_∞^+	Calculated K_∞^+
10,000	3.01×10^{-4}	4.44×10^{-4}
30,000	3.01×10^{-4}	3.76
60,000	3.01×10^{-4}	3.44

When one considers the simplicity of the assumed model, there is remarkably close agreement between the data and the calculated values. The Schmidt number dependence predicted by this particular model is however incorrect. The average mass transfer rate is actually proportional to the Schmidt number raised to a higher negative power, generally taken to be either the —2/3 or —3/4 power. This defect can be eliminated if it is assumed that eddies do not penetrate all the way to the wall (*4*). Thus it is possible that the penetration theory approach may prove to be a useful one.

The successful correlation of average velocities and average mass transfer coefficients (*12*), the partially successful correlation of the measured disturbance scales and frequency distribution with wall parameters, and the indication that the mass transfer intensity is independent of the Reynolds number all suggest that the law of the wall concept may be applied to the fluctuating velocity and concentration fields in the viscous region. On the other hand the spectra of axial velocity fluctuations, wall pressure fluctuations, and wall shear stress fluctuations correlate on a time scale based on the bulk average velocity and pipe radius. In regard to this difference the following statement by Townsend (*15*) is of interest. Near the wall "the total motion depends to some extent on the particular flow, although the universality of the relation between the mean velocity and wall stress implies that the part of the motion responsible for the shear stress is essentially the same for all flows. This motion might be called the universal motion to indicate that it behaves in the manner required by wall similarity, while the remainder of the motion, the 'irrelevant' motion, is characteristic of the particular system and does not interact with the universal motion or contribute to the Reynolds stress."

EQUATIONS GOVERNING THE CONCENTRATION FIELD

As mentioned in the introduction to this paper the surface renewal theory and the laminar film theory are both unsatisfactory in that they do not relate the mass transfer process to the flow field. One might define the goal of a theoretical treatment as follows. From a statistical description of the fluctuating flow field (or an approximate realistic model of it) one would like to be able to supply a statistical description of the rate of mass transfer over the entire solid surface. Of course one of the chief limitations toward such a theoretical approach is the lack of knowledge about the flow field in the immediate vicinity of a solid surface. Some progress is being made along these lines (*6, 9*). However at present one cannot look to the results of the research reported in this paper as a confirmation of a proper theory. Rather one must infer from them something about the flow field itself and the equations governing the process.

The interrelation between the concentration field and the fluctuating flow field can be seen by writing a differential mass balance on the diffusing substance and by representing the concentration and the velocity as the sum of time average and fluctuating terms. Since for high Schmidt numbers the concentration boundary layer is thin compared with the pipe diameter, the curvature of the pipe wall may be neglected and the mass balance may be written for a cartesian coordinate system. If one uses a dimensionless concentration based on $(C_B - C_W)$ and the definitions presented in the notation, the mass balance for the fluctuating concentration c may be written in the following dimensionless form for an incompressible, symmetrical, fully developed turbulent flow in a pipe:

$$\frac{\delta c}{\delta t^+} + \overline{U^+}\frac{\delta c}{\delta x^+} + u^+\frac{\delta \overline{C}}{\delta x^+} + v^+\frac{\delta \overline{C}}{\delta y^+} + u^+\frac{\delta c}{\delta x^+} + v^+\frac{\delta c}{\delta y^+} + w^+\frac{\delta c}{\delta z^+} - \frac{\delta}{\delta x^+}\overline{(u^+c)} - \frac{\delta}{\delta y^+}\overline{(v^+c)} = N_{Sc}^{-1}\nabla^2 c \tag{20}$$

Equation (20) can be simplified for the system studied by taking account of the results presented in this paper and in reference *12*. From average mass transfer measurements

$$\frac{\delta \overline{C}}{\delta x^+} = \frac{4K_\infty^+}{N_{Re}} \sim 10^{-7} \tag{21}$$

$$\left(\frac{\delta \overline{C}}{\delta y^+}\right)_{y^+=0} = K^+ N_{Sc} \sim 1 \tag{22}$$

The existence of very large fluctuations in the mass transfer rate would suggest that $\delta c/\delta y^+$ is not small compared with $\delta \overline{C}/\delta y^+$. In fact

$$\left(\frac{\delta c}{\delta y^+}\right)_{y^+=0} \sim \frac{(\overline{k^2})^{1/2}}{\overline{K}}\left(\frac{\delta \overline{C}}{\delta y^+}\right)_{y^+=0} \sim 0.5 \tag{23}$$

The scales of the concentration fluctuations reported in this research provide a means of estimating the magnitude of the concentration gradients. It will be assumed that

$$\frac{\delta c}{\delta x^+} \sim \frac{1}{\lambda_a^+} \sim \frac{1}{400} \tag{24}$$

$$\frac{\delta c}{\delta z^+} \sim \frac{1}{\lambda_c^+} \sim \frac{1}{3} \tag{25}$$

The above estimates suggest some simplifications in Equation (20). The term representing axial molecular diffusion $N_{Sc}^{-1}(\delta^2 c)/(\delta x^{+2})$ may be neglected compared with molecular diffusion in the z and y directions because λ_c^+ is large compared with λ_a^+ and with the thickness of the concentration boundary layer. The term $u^+(\delta \overline{C})/(\delta x^+)$ is of little importance because of the very small magnitude of $\delta \overline{C}/\delta x^+$. As a first approximation of $u^+(\delta c)/(\delta x^+)$ and $\delta/\delta x^+(\overline{u^+c})$ may be neglected compared with $\overline{U^+}(\delta c)/(\delta x^+)$ since the measurements of Reiss and Hanratty indicate $u^+/U^+ \sim 0.1$. If w^+ is of the same magnitude as u^+, then one would expect $w^+(\delta c)/(\delta z^+)$ to be an order of magnitude larger than $\overline{U^+}(\delta c)/(\delta x^+)$ and two orders of magnitude larger than $u^+(\delta c)/(\delta x^+)$. Owing to the uncertainty of the estimate of w^+ the term $\overline{U^+}(\delta c)/(\delta x^+)$ will be retained. However it appears that the fluctuating velocity u^+ plays a minor role compared with v^+ and w^+.

On the basis of the above arguments the mass balance for the concentration fluctuations around the mean concentration becomes

$$\frac{\delta c}{\delta t^+} + \overline{U^+}\frac{\delta c}{\delta x^+} + v^+\frac{\delta \overline{C}}{\delta y^+} + v^+\frac{\delta c}{\delta y^+} + w^+\frac{\delta c}{\delta z^+} - \frac{\delta}{\delta y^+}\overline{(v^+c)} = N_{Sc}^{-1}\left(\frac{\delta^2 c}{\delta y^{+2}} + \frac{\delta^2 c}{\delta z^{+2}}\right) \tag{26}$$

If the time averaged mass balance is added to the above equation, one obtains the following expression as a balance for the concentration field:

$$C = \bar{C} + c$$

$$\frac{\delta C}{\delta t^+} + \overline{U^+}\frac{\delta C}{\delta x^+} + v^+\frac{\delta C}{\delta y^+} + w^+\frac{\delta C}{\delta z^+} = N_{Sc}^{-1}\left(\frac{\delta^2 C}{\delta y^{+2}} + \frac{\delta^2 C}{\delta z^{+2}}\right) \quad (27)$$

The most important observation to be made from Equations (26) and (27) is that local fluctuations in the fully developed rate of mass transfer reflect fluctuations in the normal and circumferential velocity components of the flow field. It is of interest to note that the one term which most certainly is not important with reference to the present research, that is $u^+(\delta\bar{C})/(\delta x^+)$, is, as shown by Reiss and Hanratty (9), the term that dominates the mass transfer fluctuations at an isolated sink on a pipe wall. [This is because the gradient $(\delta\bar{C}/\delta X)$ becomes quite large as $X \rightarrow 0$.] In fact Reiss and Hanratty used their measurements to study the velocity variations u^+ near a wall.

From the above considerations a possible explanation for the small circumferential scale can be offered. One can view the fluctuations in mass transfer as being caused by random flow of material from the bulk into the region of large concentration change close to the wall. One would expect wall eddies having a scale in the y direction of the same magnitude as the thickness of the concentration boundary layer to be most effective in causing mass transfer fluctuations. If the eddy structure is such that the scales in the y and z directions are of the same magnitude, then the circumferential scale should be approximately equal to the thickness of the concentration boundary layer as has been found in this research.

ACKNOWLEDGMENT

The Ford Foundation and the American Oil Foundation provided financial support for Paul Van Shaw during the course of this investigation.

NOTATION

A = electrode of transfer surface area
a = imbedded electrode radius
C = instantaneous concentration of transferable component, may be dimensional or dimensionless with respect to $C_b - C_w$; $\bar{C}$ time averaged concentration; C_b bulk average of the fluid flowing in the pipe; C_w concentration at transfer surface
c = fluctuating component of instantaneous concentration, $C - \bar{C}$
D = molecular diffusion coefficient
d = pipe diameter
F = Faraday's constant
$F_k(n)$ = spectral density function for mass transfer fluctuations
$F_p(n)$ = spectral density function for pressure fluctuations
$F_u(n)$ = spectral density function for velocity fluctuations
$f(n)$ = integral frequency distribution function, defined by Equation (6)
I = instantaneous electrode current; $\bar{I}$ time averaged value
i = fluctuation component of the current, $I - \bar{I}$
i = as subscript, summation index
J = mass flux at transfer surface; $\bar{J}$ time averaged value
j = as subscript, summation index
K = local instantaneous mass transfer coefficient; $\bar{K}$ time averaged value
k = fluctuating component of above as measured with small but finite source; k_o true local fluctuating component
K^+ = dimensionless coefficient, $\bar{K}/U^*$
N_{Re} = Reynolds number based on pipe diameter and bulk average velocity
N_{Sc} = Schmidt number, ν/D
n = frequency
n^+ = dimensionless frequency, $n\nu/U^{*2}$
p = fluctuating pressure component
$\overline{Q^2}$ = mean square of fluctuating component of rate of mass transfer to imbedded electrode surface
q_i = fluctuating component of rate of transfer to element of imbedded electrode surface
$R, R_{1,2}$ = correlation coefficient defined by Equation (7); R_a axial; R_c circumferential
T_c = total contact time of element with the wall
t = time variable
t^+ = dimensionless time variable, tU^{*2}/ν
U = instantaneous velocity in axial direction; U_b bulk averaged value; $\bar{U}$ local time averaged value
U^* = friction velocity
u = fluctuating component of local velocity in axial direction, $U - \bar{U}$
U^+ = dimensionless instantaneous velocity in axial direction, U/U^*; $\bar{U}^+$ averaged time value
u^+ = fluctuating component of above
v = fluctuating component of velocity normal to wall
v^+ = dimensionless analogue of above, v/U^*
w = fluctuating component of velocity in circumferential direction
w^+ = dimensionless analogue of above, w/U^*
x, y, z = coordinates of a rectilinear coordinate system; x is measured from leading edge of transfer surface and runs parallel to pipe axis; y is measured from pipe wall and runs in radial direction; z runs in transverse direction
x^+, y^+, z^+ = dimensionless analogues of above, $x^+ = xU^*/\nu$ etc.
δ_c = diffusion-layer thickness
λ = scale calculated from the spatial correlation coefficients; λ_a scale in the direction of mean flow; λ_c scale in circumferential direction
ν = kinematic viscosity

LITERATURE CITED

1. Delahay, P., "New Instrumental Methods in Electrochemistry," p. 27, Interscience, New York (1954).
2. Fage, A., and H. C. H. Townend, *Proc. Roy. Soc. London*, **35A**, 636 (1932).
3. Hanratty, T. J., *A.I.Ch.E. Journal*, **2**, 359 (1956).
4. Harriot, P., *Chem. Eng. Sci.*, **17**, 149 (1962).
5. Harrison, M., *David Taylor Model Basic Hydromechanics Laboratory Research and Development Report 1260* (1958).
6. Kline, S. J., and P. W. Runstadler, *J. Appl. Mech., T.A.S.M.E.*, **26**, Series E, No. 2, p. 166 (1959).
7. Laufer, J., *NACA Tech. Rept. 1053* (1962).
8. Reiss, L. P., and T. J. Hanratty, *A.I.Ch.E. Journal*, **8**, 245 (1962).
9. *Ibid.*, **9**, 154 (1963).
10. Sanborn, V. A., *NACA Tech. Note 3266* (1955).
11. Shaw, P. V., Ph.D. thesis, University of Illinois, Urbana, Illinois (1963).
12. ———, T. J. Hanratty, and L. P. Reiss, *A.I.Ch.E. Journal*, **9**, 362 (1963).
13. Sternberg, J., *J. Fluid Mech.*, **13**, No. 2, p. 241 (1963).
14. Toor, H. L., and J. M. Marchello, *A.I.Ch.E. Journal*, **4**, 97 (1958).
15. Townsend, A. A., "The Turbulent Boundary Layer," Boundary Layer Research Symposium, H. Görtler, ed., Springer-Verlag, Germany (1958).

Manuscript received July 3, 1963; revision received December 5, 1963; paper accepted December 9, 1963.